Supporting Information for

The impact of hydrothermal vent geochemistry on the addition of iron to the deep ocean

Alastair J. M. Lough[1,*], Alessandro Tagliabue[2], Clement Demasy[1], Joseph A. Resing[3], Travis Mellett[4], Neil J. Wyatt[1], Maeve C. Lohan[1]

[1]Ocean & Earth Science, University of Southampton, Southampton, SO14 3ZH, UK
[2]Earth, Ocean & Ecological Sciences, Liverpool, L69 3BX, UK
[3]Cooperative Institute for Climate, Oceans, and Ecosystem Studies, University of Washington and NOAA-PMEL, Seattle, USA
[4]University of South Florida, St. Petersburg, FL, FL 33701, United States.

<u>Contents of this file</u>

Table S1. Extended summary of plume dFe/xs^{3}He ratios over vent sites and for repeat sampling at TAG and Rainbow using different methods to calculate dFe/xs3He. The young rising plume was identified over Rainbow as a narrow spike in TDFe, dFe, xs3He and dMn close to the seafloor (Supplementary Information, Figure S8). This signal is separated as these samples will be from a cross section of the young rising plume as the CTD rosette passed through it.

	Plume integrated dFe/xs^{3}He (nmole/fmole) values		dFe/xs^{3}He (nmole/fmole) from slope of regression	
Site	Integrated from separate casts (Method 1)	Dual-Mn method (Method 2)	Interpolation method (Method 3)	
			slope	r^2
Menez Gwen	5	12	6	1
Lucky Strike	26	4	-10	0.901
Lucky Strike	ND	8	ND	
Rainbow	49	12	132	0.233
Rainbow	34	44	-197	0.997
Rainbow*	63	4	ND	
TAG	4	7	0.1	0.003
TAG	87	86	113	0.538
TAG	ND	4	ND	
Close E Rainbow (33 km)	5	4	15	0.479
Close W Rainbow (30 km)	8	8	10	0.132
Close N Rainbow (34 km)	15	8	-7	1
S of Rainbow (39 km)	11	6	11	0.099
Close S of Rainbow (10 km)	ND	6	ND	

N of Rainbow (25 km)	20	15	-16	-0.128
Close N of TAG (29 km)	ND	9	31	0.101
Close S of TAG (30 km)	ND	4	-1	-0.140
Close W of TAG (30 km)	30	38	512	-0.211
Close E of TAG (30 km)	ND	4	-8	-0.270
Close N of TAG (18 km)	ND	6	26	0.416

ND = no data, either no dMn data available from the trace metal rosette or no ^{3}He data available from the stainless-steel rosette at the equivalent depth.

***The young rising plume was identified over Rainbow close to the seafloor with density lower than that of other stations at the same depth (Supplementary Information, Figure S8 and S10). This signal is separated as these samples will be from a cross section of the young rising plume as the CTD rosette passed through it.).**

Method 3. Interpolation method: Interpolate the distinct dFe and xs3He data in the depth profile to create a matchup between both the variables and calculate the dFe/xs3He using linear regression (Saito et al., 2013) – this assumes that any change in concentration between sampled depths is linear and there are not any additional sources of variability. Note that Saito et al. (2013) did not measure xs^{3}He but used data from a separate cruise then interpolated this for dFe sample depths and location. Saito et al. (2013) account for differences in water mass distribution between separate casts on separate cruises using optimum multi-parameter analysis. We did not do this when using this interpolation method as our separate casts were typically taken within 24 hours of each other so there was minimal change in water mass contributions with depth.

The estimated ratios from interpolation are so variable compared to the other methods of estimation. Largely because of the variability introduced by the interpolation method (often producing negative dFe/xs^{3}He ratios) as the shape of the plume depth profile (for both xs^{3}He and dFe) or the age of the plume is not reproducible between trace metal clean and standard sampling casts (Figure 2, Figure S2 and S4) at the high spatial sampling resolution of this study.

Figures

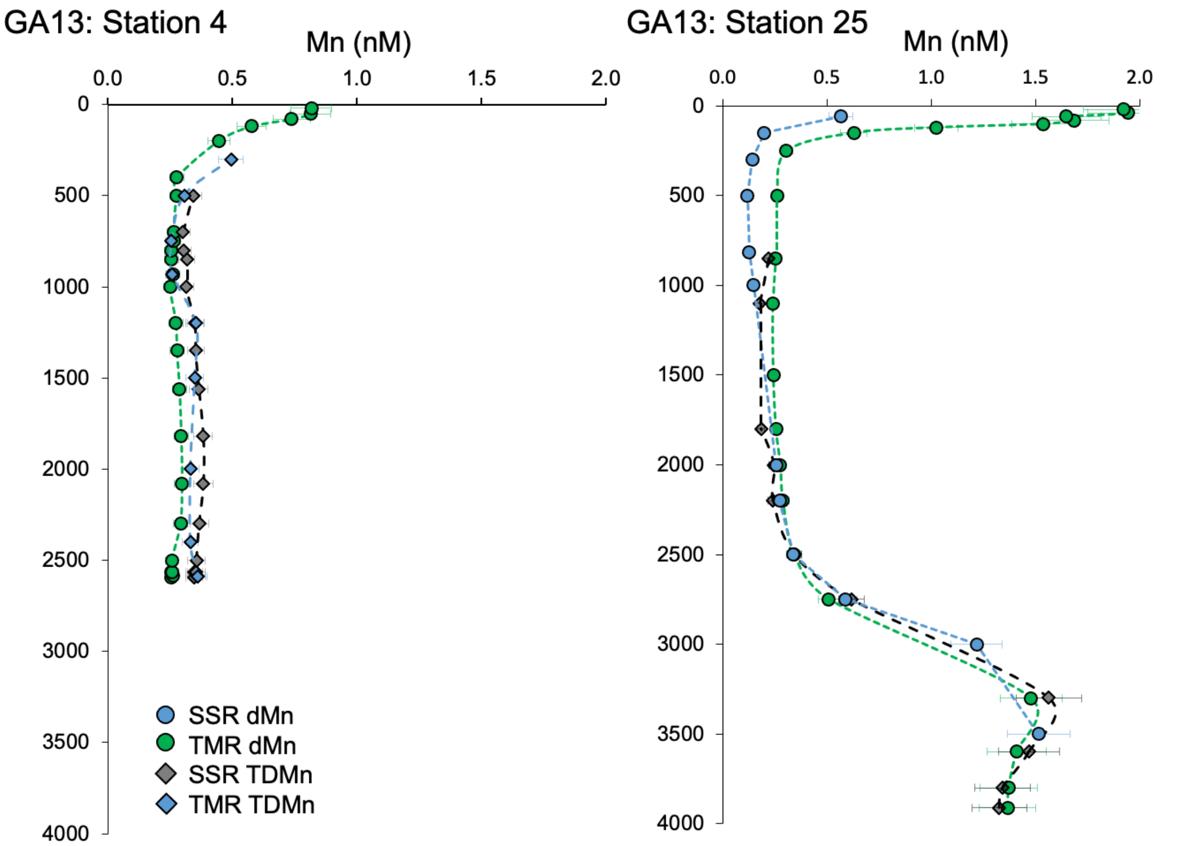

Figure S1. Comparison of dissolved and total dissolvable Mn data between the standard stainless steel (SSR) and trace metal clean (TMR) Niskin rosettes at stations where there is Mn data for both. Overlap of profiles indicates Mn can be sampled cleanly from the stainless-steel rosette without risk of contamination as can be seen from these profiles with similar Mn concentrations to background N. Atlantic seawater. In this example all samples were measured by flow injection. We note a ~0.2 nM discrepancy between dMn measurements I surface waters at station 25 however this is unlikely to impact our assessment of the data which excludes samples shallower than 600 m.

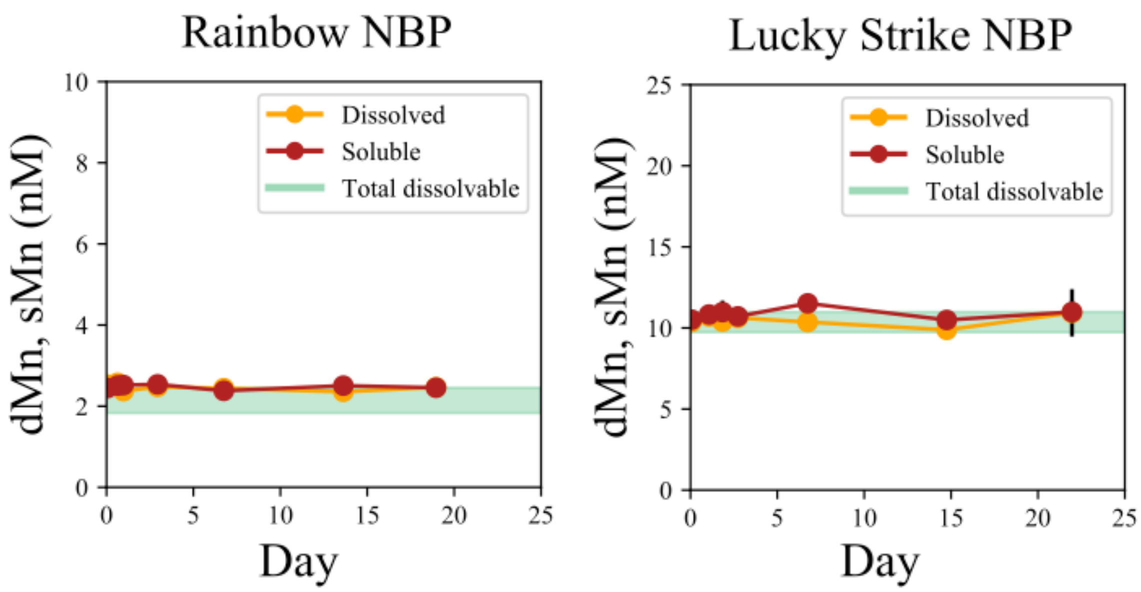

Figure S2. Dissolved, soluble, and total dissolvable manganese (Mn) concentrations in an incubation experiment on Rainbow and Lucky Strike unfiltered neutrally buoyant plume waters. Presented are the soluble (<0.02 μm) fraction (red circles) and dissolved (<0.2 μm) fraction (yellow circles) concentrations for Mn. The green band represents the average ± the standard deviation of all total dissolvable (unfiltered, acidified) from every sample taken in the incubation. Demonstrating the dMn is conservative within the time frame that it takes plume water to escape the Ridge valley (Vic et al., 2018). Data are taken from Mellett et al. (in prep)

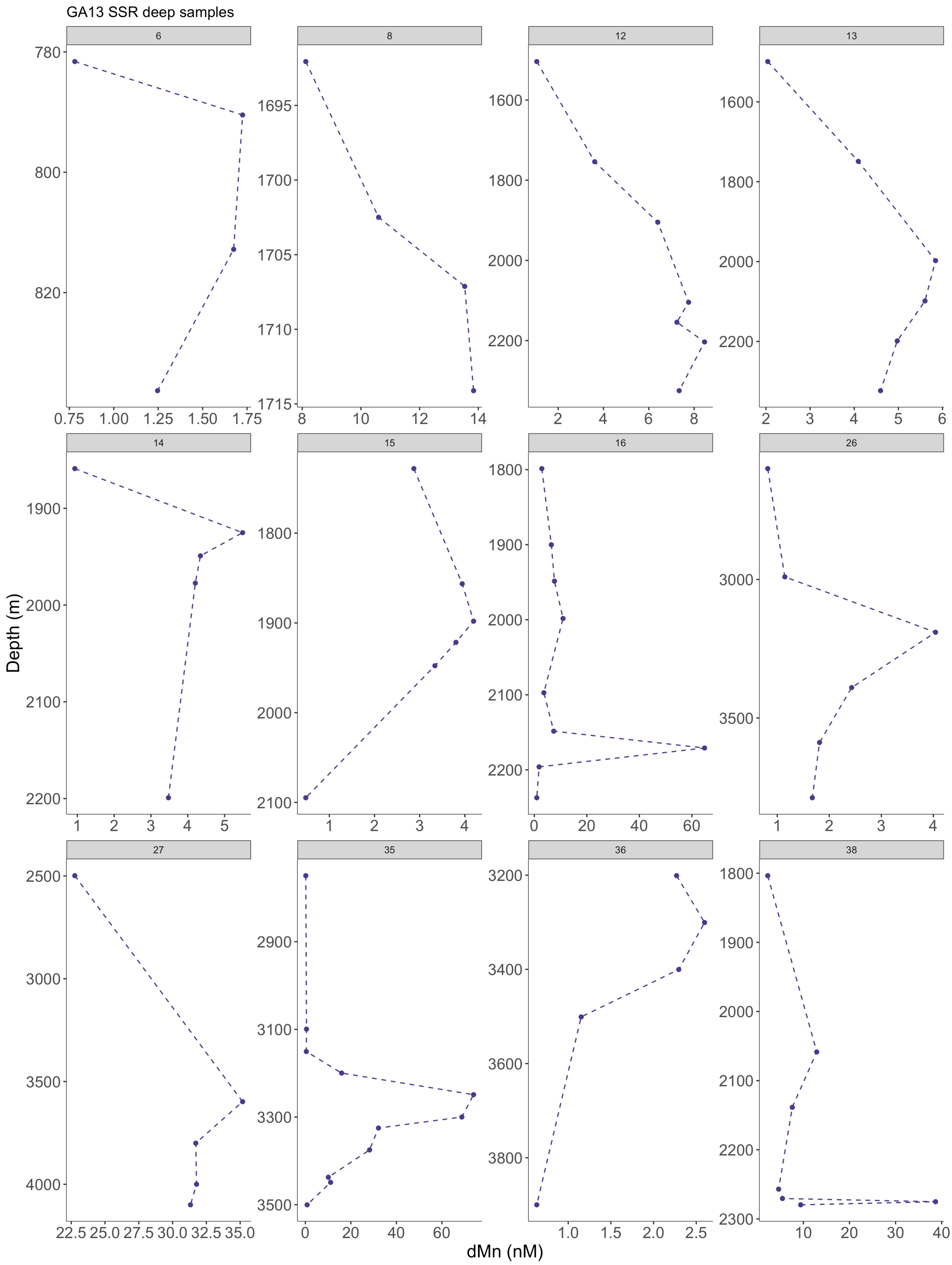

Figure S3. Dissolved Mn data from the standard (stainless-steel) rosette cast at each station (grey box's), where dMn >0.15 nM N. Atlantic background value and neutral density >27 mg/kg. Main casts over vent sites are 6 = Menez Gwen, 8 = Lucky Strike, 16 and 38 = Rainbow, 35 and 36 = TAG.

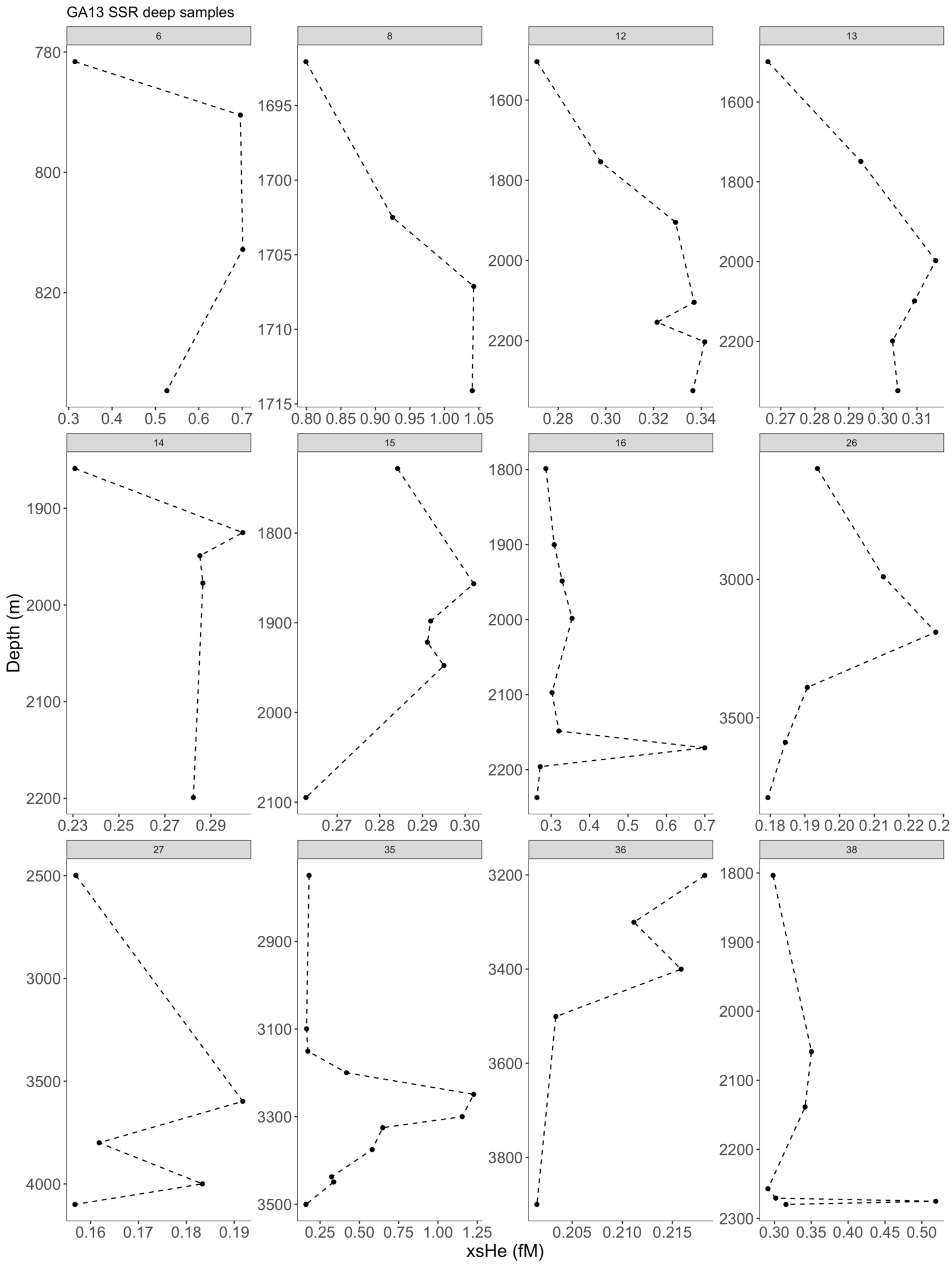

Figure S4. xs^{3}He data from the stainless-steel rosette cast at each station (grey box's), where dMn >0.15 nM N. Atlantic background value and neutral density >27 mg/kg. Main casts over vent sites are 6 = Menez Gwen, 8 = Lucky Strike, 16 and 38 = Rainbow, 35 and 36 = TAG.

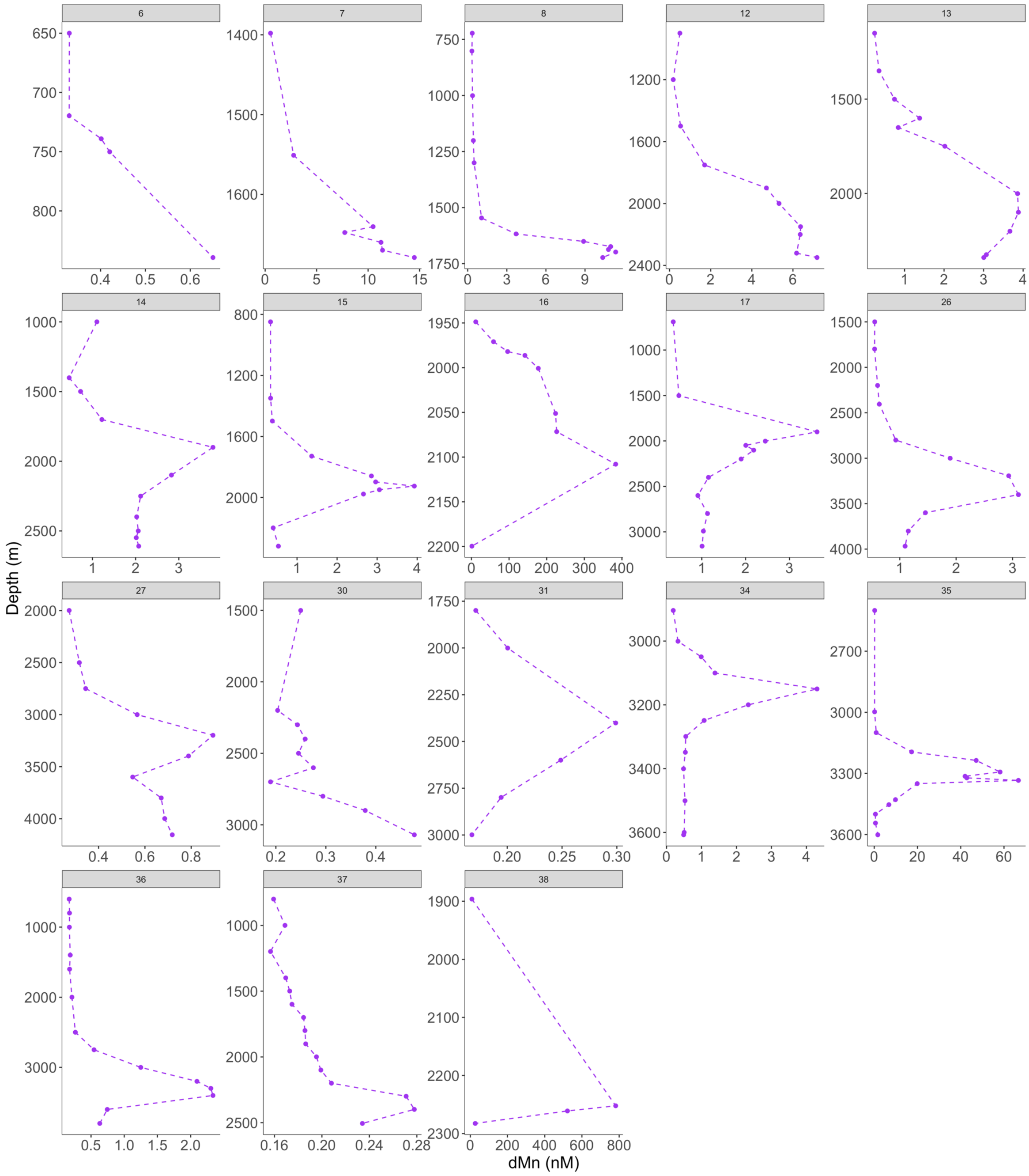

Figure S5. dMn data from the trace metal clean rosette cast at each station (grey box's), where dMn >0.15 nM and dFe >0.5 nM N. Atlantic background values and neutral density > 27 mg/kg. The dMn data is used with the slope values from Figure 3A to derive "xsHe$_{Mn}$" shown in Figure S5 and Figure 4. Main casts over vent sites are 6 = Menez Gwen, 7 and 8 = Lucky Strike, 16 and 38 = Rainbow, 35 and 36 = TAG.

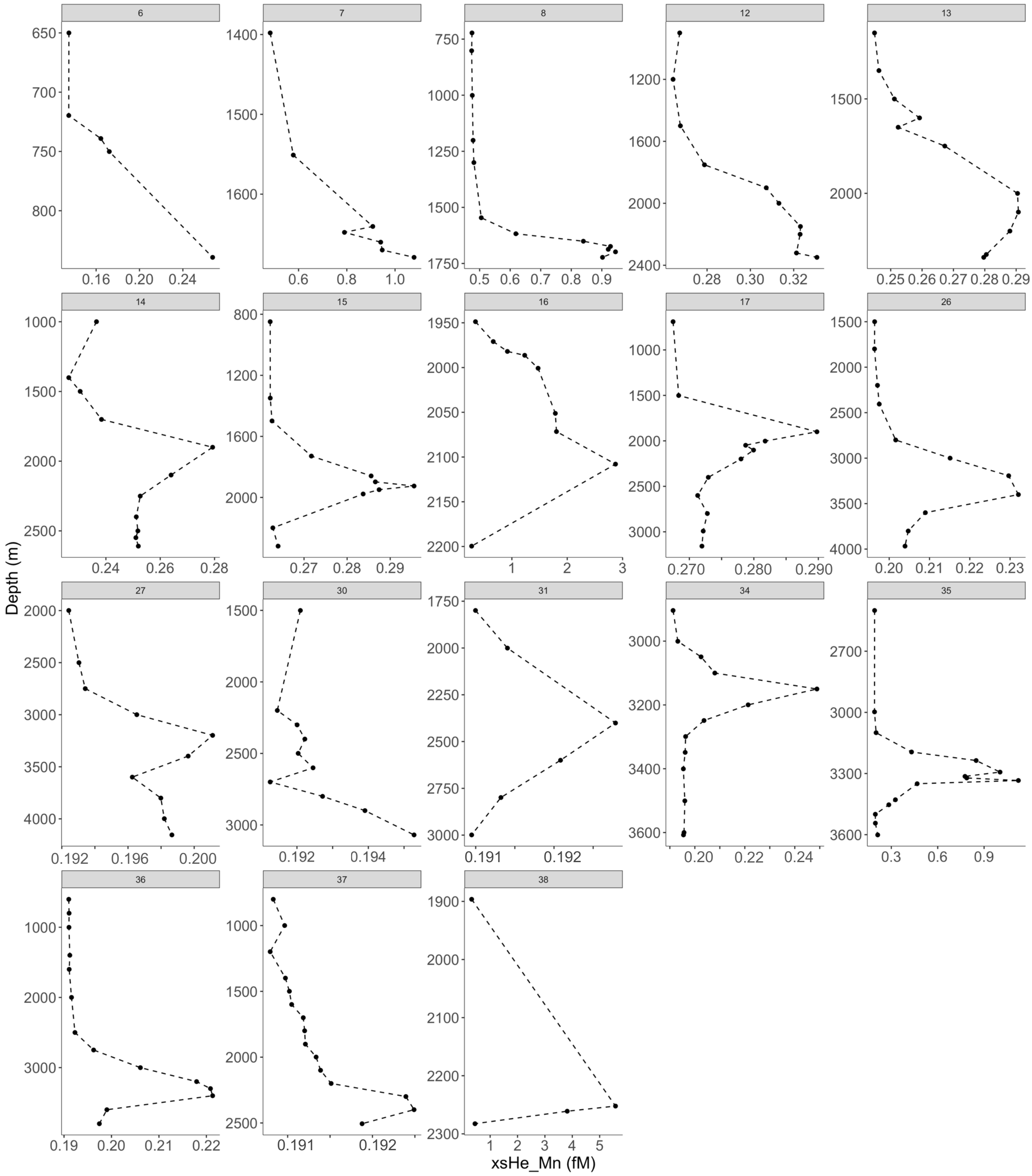

Figure S6. Derived xs^3He_{Mn} values for the trace metal clean rosette cast at each station (grey box's), where dMn >0.15 nM and dFe >0.5 nM N. Atlantic background value and neutral density >27 mg/kg. The xs^3HeMn data is calculated from the slope values shown on Figure 3A. Main casts over vent sites are 6 = Menez Gwen, 7 and 8 = Lucky Strike, 16 and 38 = Rainbow, 35 and 36 = TAG.

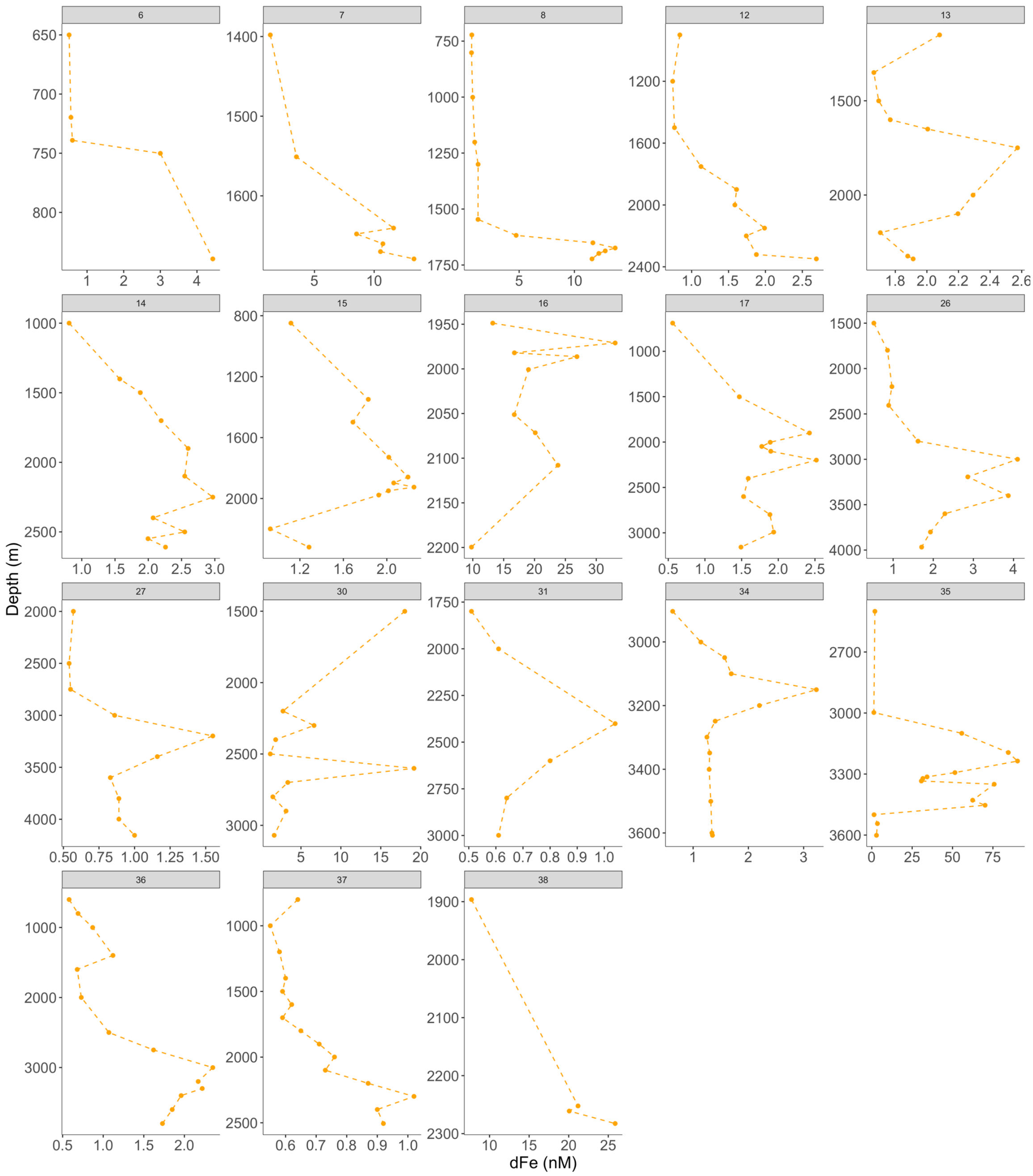

Figure S7. Dissolved Fe data (for the trace metal clean rosette cast) used for integration at each station (grey box's), where dMn >0.15 nM and dFe >0.5 nM N. Atlantic background value and neutral density >27 mg/kg. Main casts over vent sites are 6 = Menez Gwen, 7 and 8 = Lucky Strike, 16 and 38 = Rainbow, 35 and 36 = TAG.

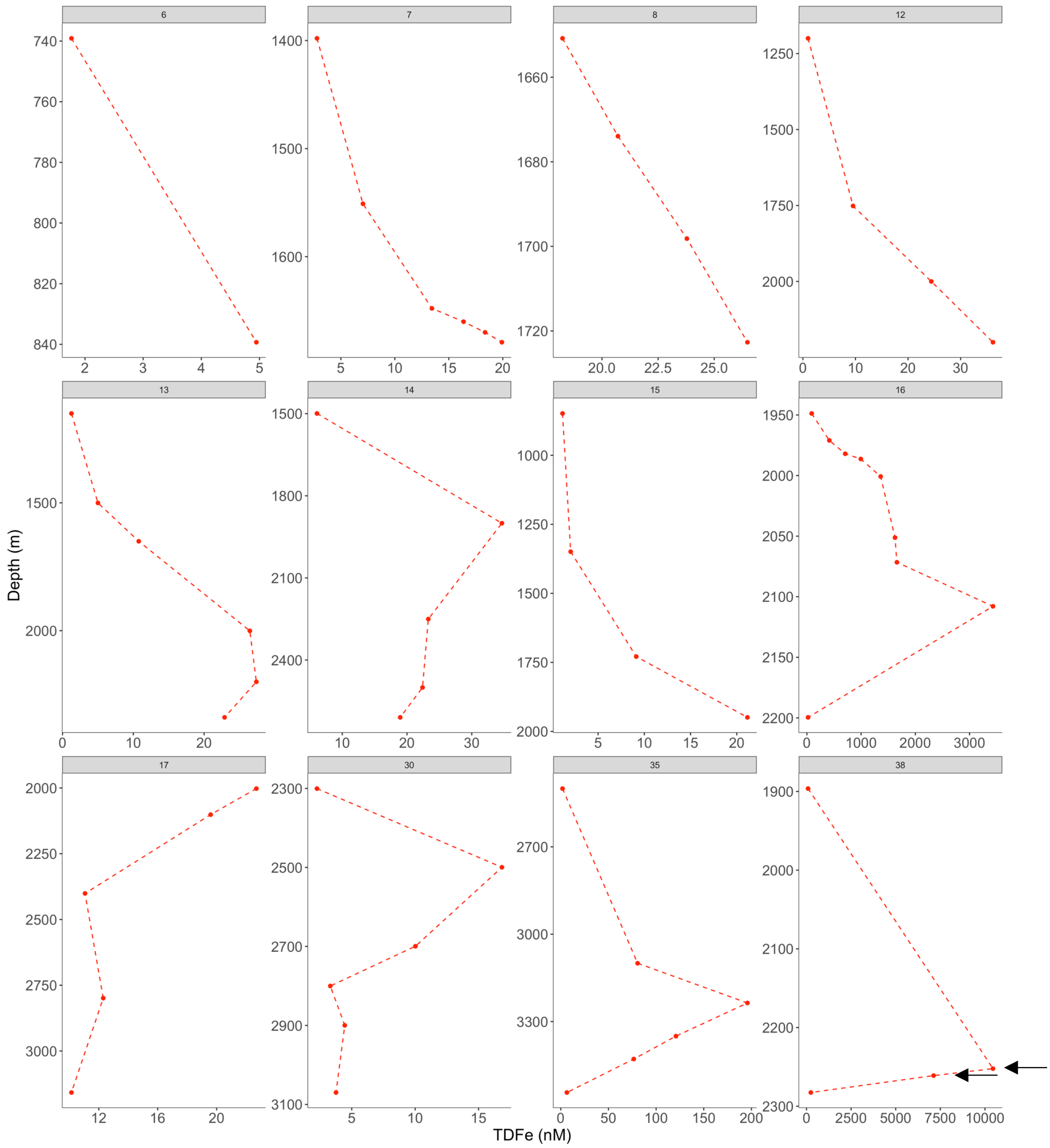

Figure S8. Total dissolvable Fe data (for the trace metal clean rosette cast) used for integration at each station (grey box's), where dMn >0.15 nM and dFe >0.5 nM N. Atlantic background value and neutral density >27 mg/kg. Black arrows indicate young buoyant plume samples identified by high TDFe concentration, negative Eh, and ND anomaly (lower ND at same depth relative to background). These points were integrated separately (for sFe, dFe and TDFe) so as not to overestimate integrated values. Had more samples been collected between 2200 and 1900 m at station 38 we anticipate TDFe concentrations would of returned to the 1 – 1000 nM range observed at station 16. Main casts over vent sites are 6 = Menez Gwen, 7 and 8 = Lucky Strike, 16 and 38 = Rainbow, 35 and 36 = TAG.

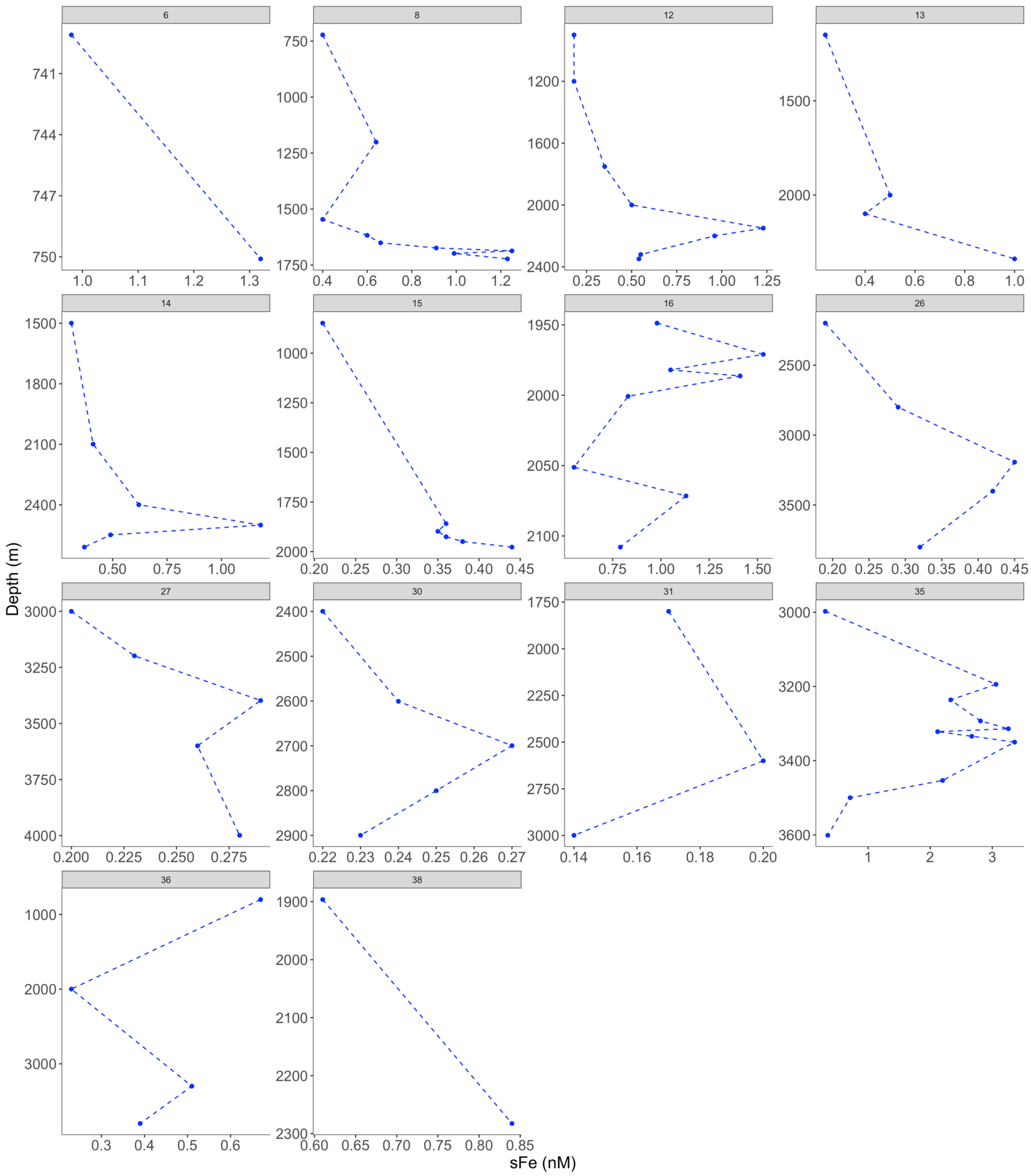

Figure S9. Soluble Fe data (for the trace metal clean rosette cast) used for integration at each station (grey box's), where dMn >0.15 nM and dFe >0.5 nM N. Atlantic background value and neutral density >27 mg/kg. Main casts over vent sites are 6 = Menez Gwen, 8 = Lucky Strike, 16 and 38 = Rainbow, 35 and 36 = TAG.

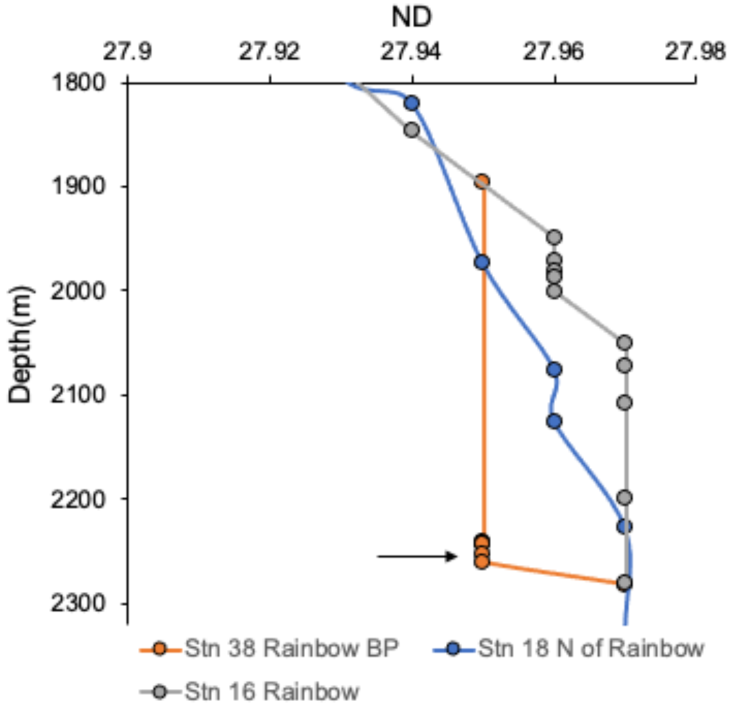

Figure S10. Comparison of neutral density (ND (kg/m^3) profiles at 3 stations around Rainbow. The black arrow indicates samples from station 38 over Rainbow classified as being within the buoyant plume, as the density is lower than that of the other stations at the equivalent depth near the seafloor. These samples are the same as those highlighted by the black arrow in figure S7 that had the highest observed TDFe concentrations.

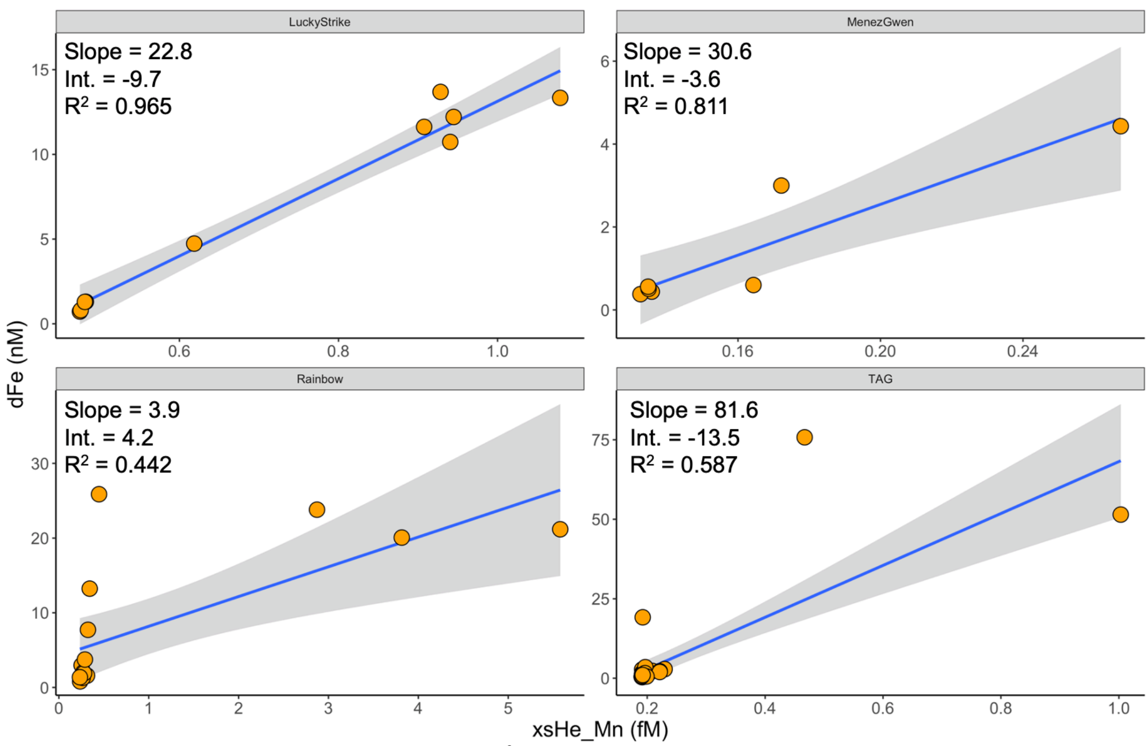

Figure S11. Linear regression statistics for dFe/xs^{3}He$_{Mn}$ relationship at each vent site using individual sample points (i.e. not integrated profiles which is what the main text focuses on).

References

Mellett, T., Albers, J., Wang, W., Lough, A. J. M., Santoro, A., Bundy, R. M., Lohan, M., Tagliabue, A., and Buck, K. N.: Particulate and dissolved iron exchange mediated by organic ligands in hydrothermal vent plumes along the Mid-Atlantic Ridge, in prep.

Saito, M. A., Noble, A. E., Tagliabue, A., Goepfert, T. J., Lamborg, C. H., and Jenkins, W. J.: Slow-spreading submarine ridges in the South Atlantic as a significant oceanic iron source, Nat. Geosci., 6, 775-779, 10.1038/ngeo1893, 2013.

Vic, C., Gula, J., Roullet, G., and Pradillon, F.: Dispersion of deep-sea hydrothermal vent effluents and larvae by submesoscale and tidal currents, Deep Sea Research Part I: Oceanographic Research Papers, 1-51, 2018.